RESEARCH ARTICLES

New Method for Characterizing Dissolution Properties of Drug Powders

PETER VENG PEDERSEN

Abstract □ Various multiparticulate dissolution models that assume a log-normal particle-size distribution are fitted by nonlinear least-squares regression to data from the dissolution of micronized glyburide. Estimates of parameters describing the effective initial particle-size distribution are obtained, together with estimates of the specific dissolution rate parameter. A dissolution equation based on an ideal, untruncated, log-normal distribution, with the single particles dissolving according to the Hixson–Crowell cube root law, is the best model. The dissolution behavior of glyburide can be well described by this model in terms of the specific dissolution rate parameter and one other parameter accounting for the distribution effect. The estimation of these two parameters represents a more exact way of describing the dissolution characteristics of drug powders than previous approaches. The method should be of interest in the quality control of drugs that may cause bioavailability problems because of dissolution rate-limited absorption.

Keyphrases □ Dissolution—micronized glyburide, various multiparticulate models fit to data, rate and size distribution parameters evaluated □ Powders—micronized glyburide, various multiparticulate models fit to dissolution data, rate and size distribution parameters evaluated □ Glyburide, micronized—dissolution, various multiparticulate models fit to data, rate and size distribution parameters evaluated

The dissolution behavior of a multiparticulate system is determined by the single-particle dissolution behavior and the particle-size distribution (1, 2). Dissolution profiles have been related to the initial particle-size distribution (3, 4). However, the mathematical models used to account for the size distribution effect were not exact but were based on empirical approximations.

A previous paper (5) showed good agreement between the theoretical dissolution profile based on a rigorous mathematical treatment and dissolution data for tolbutamide. The present paper evaluates some kinetic models for multiparticulate dissolution by fitting them to data from the dissolution of micronized glyburide. This method represents a new and better approach for characterizing the dissolution behavior of powders by evaluating both rate and size distribution parameters. The method should be of value in quality control measurements of slightly soluble pure drugs that can cause bioavailability problems.

THEORY

Consider a multiparticulate dissolution where the single particles dissolve according to the Hixson–Crowell (6) cube root law or the Niebergall et al. (7) square root law, which can be written in a common form as:

$$w^{1/m} = w_0^{1/m} - k_m t \qquad \text{(Eq. 1)}$$

where $m = 3$ for the cube root law and $m = 2$ for the square root law[1].

Let the initial effective particle diameters, a_0, be log normally distributed, i.e., have a frequency distribution that is well approximated by the following density distribution (2):

$$\mu(\ln a_0) = \frac{N(\ln a_0, \mu, \sigma)}{\int_{\ln a_0 = \mu - i\sigma}^{\ln a_0 = \mu + j\sigma} N(\ln a_0, \mu, \sigma) d \ln a_0} \qquad \text{(Eq. 2)}$$

for $\mu - i\sigma \leq \ln a_0 \leq \mu + j\sigma$ where i and j are the lower and upper truncation parameters (Fig. 1), and N is the normal density function defined by:

$$N(x, \mu, \sigma) = \frac{1}{\sigma \sqrt{2\pi}} e^{-\frac{1}{2}\left(\frac{x - \mu}{\sigma}\right)^2} \qquad \text{(Eq. 3)}$$

The dissolution of such a multiparticulate powder is described by (2):

$$\frac{W}{W_0} = \sum_{n=0}^{m} \binom{m}{n} (-K_m t)^{(m-n)}$$

$$\times \frac{F\left(\frac{T_2 - \mu}{\sigma} - \frac{3n\sigma}{m}\right) - F\left(\frac{T_1 - \mu}{\sigma} - \frac{3n\sigma}{m}\right)}{F(j - 3\sigma) - F(-i - 3\sigma)} e^{3(n-m)[\mu + 3(n+m)\sigma^2/2m]/m}$$

(Eq. 4)

---

[1] The positive constants k_3 ($m = 3$) and k_2 ($m = 2$) are used for simplicity to replace the coefficients of time that contain quantities such as density, the diffusion coefficient, and the shape factor, which are considered constant.
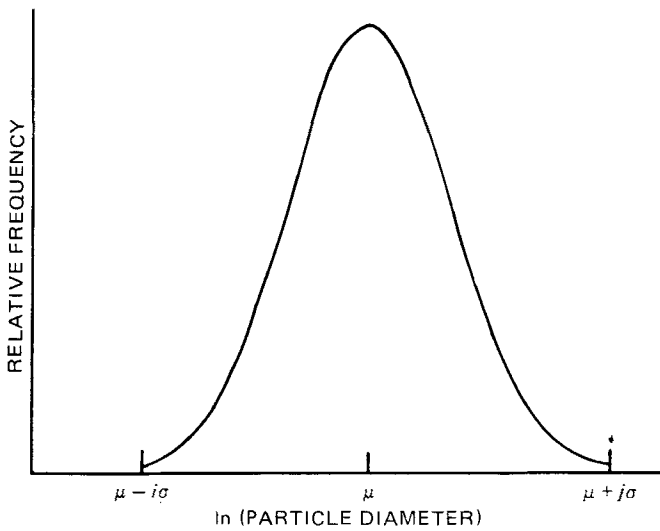
Figure 1—*Illustration of the initial (t = 0) particle-size distribution parameters, μ, σ, i, and j, of a log-normal powder. The approximating distribution function shown is defined in Eq. 2. The initial diameters, a_0, are diameters of hypothetical spherical particles that approximate the dissolution behavior of the real nonspherical particles. The dimensionless distribution shape parameters, i, j, and σ, can be estimated from the dissolution profile (Figs. 3–6) by nonlinear least-squares regression analysis (Table I). The scale parameter, μ, cannot be determined.*

where W/W_0 is the fraction of undissolved powder at time t, F is the cumulative standard normal distribution function defined by:

$$F(x) = \frac{1}{\sqrt{2\pi}} \int_{-\infty}^{x} e^{-x^2/2}\, dx \qquad \text{(Eq. 5)}$$

T_1 and T_2 are given by:

$$T_1 = \mu - i\sigma \qquad \text{for } \frac{m}{3} \ln (K_m t) < \mu - i\sigma \qquad \text{(Eq. 6)}$$

$$T_1 = \frac{m}{3} \ln (K_m t) \qquad \text{for } \frac{m}{3} \ln (K_m t) \geq \mu - i\sigma \qquad \text{(Eq. 7)}$$

$$T_2 = \mu + j\sigma \qquad \text{for } \frac{m}{3} \ln (K_m t) < \mu + j\sigma \qquad \text{(Eq. 8)}$$

$$T_2 = \frac{m}{3} \ln (K_m t) \qquad \text{for } \frac{m}{3} \ln (K_m t) \geq \mu + j\sigma \qquad \text{(Eq. 9)}$$

and:

$$\binom{m}{n} = \frac{m!}{(m-n)!n!} \qquad \text{(Eq. 10)}$$

If the particles are spherical, K_m is related to k_m by:

$$K_m = (6/\rho\pi)^{1/m} k_m \qquad \text{(Eq. 11)}$$

Equation 4 appears to contain five parameters, namely, σ, i, j, μ, and K_m, which define the dissolution profile (W/W_0 *versus* time). However, an attempt to obtain least-squares estimates of all five parameters from W/W_0 *versus* time data may fail, because μ and K_m can be fused into a single rate parameter:

$$K_m^* = e^{-3\mu/m} K_m \qquad \text{(Eq. 12)}$$

which will be called the specific dissolution rate parameter.

The uniqueness of these four parameters, σ, i, j, and K_m^*, in defining the dissolution profile can be seen by substituting $K_m = e^{3\mu/m}K_m^*$ into Eq. 4, resulting in total cancellation of μ, in full agreement with the theory discussed previously (2):

$$\frac{W}{W_0} = \sum_{n=0}^{m} \binom{m}{n} (-K_m^* t)^{(m-n)} \frac{F\left(j - \frac{3n\sigma}{m}\right) - A}{F(j - 3\sigma) - F(-i - 3\sigma)} e^{2[(n/m)^2-1]\sigma^2/9} \qquad \text{(Eq. 13)}$$

where:

$$A = F\left(-i - \frac{3n\sigma}{m}\right) \qquad \text{for } t < \frac{1}{K_m^*} e^{-3i\sigma/m} \qquad \text{(Eq. 14)}$$

and:

$$A = F\left[\frac{m}{3\sigma} \ln (K_m^* t) - \frac{3n\sigma}{m}\right] \qquad \text{for } \frac{1}{K_m^*} e^{3j\sigma/m} > t > \frac{1}{K_m^*} e^{-3i\sigma/m} \qquad \text{(Eq. 15)}$$

and:

$$\frac{W}{W_0} = 0 \qquad \text{for } t \geq \frac{1}{K_m^*} e^{3j\sigma/m} \qquad \text{(Eq. 16)}$$

The continuously recording flow-through dissolution apparatus used provides dissolution rate data. The fraction undissolved, W/W_0, *versus* time can be obtained by integrating these data (5). The parameters σ, i, j, and K_m^* can then be estimated by nonlinear least-squares regression analysis using Eq. 13. However, the integrated data contain integration errors. The integration also tends to "smooth" the original data, so estimates of the variability of the parameters will be less reliable than if the original rate data were used. Therefore, it is useful to derive an expression for the release rate to estimate the four parameters directly from the original (rate) data.

By applying Eq. 13a of Ref. 1, the following equation (similar to Eq. A2 in the same reference) is obtained:

$$\frac{W}{W_0} = \frac{\int_{R_1}^{R_2} (x^{3/m} - K_m t)^m x^{-1} N(\ln x, \mu, \sigma)\, dx}{\int_{d_0}^{D_0} x^2 N(\ln x, \mu, \sigma)\, dx} \qquad \text{(Eq. 17)}$$

where:

$$d_0 = e^{\mu - i\sigma} \qquad \text{(Eq. 18)}$$

$$D_0 = e^{\mu + j\sigma} \qquad \text{(Eq. 19)}$$

$$R_1 = d_0 \qquad \text{for } K_m t < d_0^{3/m} \qquad \text{(Eq. 20)}$$

$$R_1 = (K_m t)^{m/3} \qquad \text{for } K_m t \geq d_0^{3/m} \qquad \text{(Eq. 21)}$$

$$R_2 = D_0 \qquad \text{for } K_m t < D_0^{3/m} \qquad \text{(Eq. 22)}$$

$$R_2 = (K_m t)^{m/3} \qquad \text{for } K_m t \geq D_0^{3/m} \qquad \text{(Eq. 23)}$$

An expression for the dissolution rate of drug, $Q = -dW/dt$, can now be found by differentiating Eq. 17 with respect to time (using Leibnitz's rule). For abbreviation, let B denote the (constant) denominator of Eq. 17; differentiation then gives:

$$\frac{B}{W_0} Q = mK_m \int_{R_1}^{R_2} (x^{3/m} - Kt)^{(m-1)} x^{-1} N(\ln x, \mu, \sigma)\, dx$$
$$- (R_2^{3/m} - K_m t)^m R_2^{-1} N(\ln R_2, \mu, \sigma)\, \frac{dR_2}{dt}$$
$$+ (R_1^{3/m} - K_m t)^m R_1^{-1} N(\ln R_1, \mu, \sigma)\, \frac{dR_1}{dt} \qquad \text{(Eq. 24a)}$$

Before the critical time[2], $R_1 = d_0$ and $R_2 = D_0$, so $dR_1/dt = dR_2 dt = 0$ and the last two terms of the right-hand side of Eq. 24a vanish. After the critical time, dR_2/dt is still zero, but $R_1 = (K_m t)^{m/3}$ (according to Eq. 21). Thus, the last term also vanishes because:

$$R_1^{3/m} - K_m t = [(K_m t)^{m/3}]^{3/m} - K_m t = 0 \qquad \text{(Eq. 24b)}$$

Equation 24a can be simplified to:

$$Q = mK_m W_0 \frac{\int_{R_1}^{R_2} (x^{3/m} - K_m t)^{(m-1)} x^{-1} N(\ln x, \mu, \sigma)\, dx}{\int_{d_0}^{D_0} x^2 N(\ln x, \mu, \sigma)\, dx} \qquad \text{(Eq. 25)}$$

The term $(x^{3/m} - K_m t)^{(m-1)} x^{-1}$ under the integral sign can be expanded:

$$(x^{3/m} - K_m t)^{(m-1)} x^{-1}$$
$$= x - 2K_3 t + (K_3 t)^2 x^{-1} \qquad \text{(for } m = 3) \qquad \text{(Eq. 26)}$$

$$(x^{3/m} - K_m t)^{(m-1)} x^{-1} = x^{1/2} - K_2 t x^{-1} \qquad \text{(for } m = 2) \qquad \text{(Eq. 27)}$$

and a formula given previously (Eq. A3 of Ref. 1) can be applied to express the integrals in Eq. 25 in terms of the function F (Eq. 5). This process leads to the following expression for Q that can be evaluated more readily

---

[2] The critical time is the time when the first particles start disappearing in the dissolution process, *i.e.*, $t = (1/K_m)e^{3/m(\mu-i\sigma)}$.
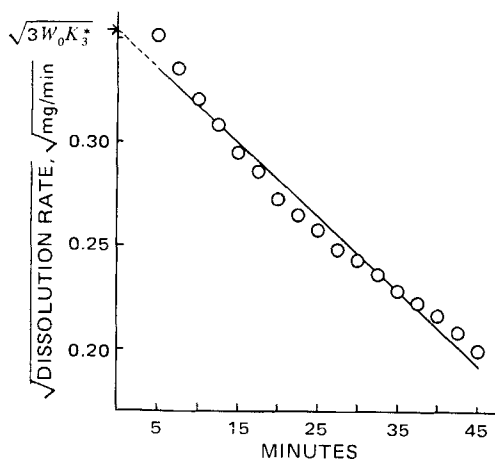
Figure 2—*Illustration of a graphic method for obtaining an initial estimate of the specific dissolution rate parameter, K_m^*, from rate data from the dissolution of 5 mg of micronized glyburide. Equation 39 predicts a linear relationship between $\sqrt{Q}$ and t for a monodisperse powder in which the single particles dissolve according to the cube root law (Eq. 1, m = 3). The deviation from linearity in the graph is caused by the particle-size distribution effect.*

and exactly than Eq. 25:

$$Q = mK_mW_0 \sum_{n=0}^{(m-1)} \binom{m-1}{n} (-K_mt)^{(m-n-1)}$$

$$\times \frac{F\left(\dfrac{T_2 - \mu}{\sigma} - \dfrac{3n\sigma}{m}\right) - F\left(\dfrac{T_1 - \mu}{\sigma} - \dfrac{3n\sigma}{m}\right)}{F(j - 3\sigma) - F(-i - 3\sigma)} e^{3(n-m)[\mu+3(n+m)\sigma^2/2m]/m}$$

(Eq. 28)

where T_1 and T_2 are as defined previously (Eqs. 6–9).

This expression for the dissolution rate, Q, contains five parameters $(\sigma, i, j, \mu, \text{and } K_m)$. However, as before (Eq. 13), only four parameters $(\sigma, i, j, \text{and } K_m^*)$ are needed to define uniquely the dissolution rate profile:

$$Q = mK_m^*W_0 \sum_{n=0}^{(m-1)} \binom{m-1}{n} (-K_m^*t)^{(m-n-1)}$$

$$\times \frac{F\left(j - \dfrac{3n\sigma}{m}\right) - A}{F(j - 3\sigma) - F(-i - 3\sigma)} e^{9[(n/m)^2-1]\sigma^2/2} \quad \text{(Eq. 29)}$$

This equation is the differential form of Eq. 13.

The quantity A is as defined previously (Eqs. 14 and 15) and $Q = 0$ for $t \geq (1/K_m^*) e^{3j\sigma/m}$. This expression is valuable since it allows the effective initial particle-size distribution parameters, $\sigma, i, \text{and } j$, to be determined together with the specific dissolution rate parameter, K_m^*, by nonlinear regression analysis of the dissolution rate profile (dW/dt versus time).

It is also of interest to investigate how well the dissolution behavior can be described if the particle-size distribution is considered ideal, i.e., if $i = j = \infty$. With $F(\infty) = 1$ and $F(-\infty) = 0$, Eq. 29 becomes, for an ideal distribution:

$$Q = mK_m^*W_0 \sum_{n=0}^{(m-1)} \binom{m-1}{n} (-K_m^*t)^{(m-n-1)}$$

$$\times \left\{1 - F\left[\frac{m}{3\sigma} \ln(K_m^*t) - \frac{3n\sigma}{m}\right]\right\} e^{9[(n/m)^2-1]\sigma^2/2} \quad \text{(Eq. 30)}$$

If the distribution is considered ideal at the lower end ($i = \infty$) but truncated at the higher end, the expression becomes:

$$Q = mK_m^*W_0 \sum_{n=0}^{(m-1)} \binom{m-1}{n} (-K_m^*t)^{(m-n-1)}$$

$$\times \frac{F\left(j - \dfrac{3n\sigma}{m}\right) - F\left[\dfrac{m}{3\sigma} \ln(K_m^*t) - \dfrac{3n\sigma}{m}\right]}{F(j - 3\sigma)} e^{9[(n/m)^2-1]\sigma^2/2} \quad \text{(Eq. 31)}$$

and if it is considered truncated at the lower end but not at the higher end ($j = \infty$):

$$Q = mK_m^*W_0 \sum_{n=0}^{(m-1)} \binom{m-1}{n} (-K_m^*t)^{(m-n-1)}$$

$$\times \frac{1 - A}{1 - F(-i - 3\sigma)} e^{9[(n/m)^2-1]\sigma^2/2} \quad \text{(Eq. 32)}$$

Discussion of the limiting case where the particle-size distribution is infinitely narrow, i.e., $\sigma = 0$, allows a better understanding of the specific dissolution rate parameter, K_m^*. It also provides a method of obtaining a suitable initial estimate of this parameter to use in nonlinear curve fitting.

When $\sigma = i = j = 0$, Eq. 29 becomes:

$$Q = mK_m^*W_0 \sum_{n=0}^{(m-1)} \binom{m-1}{n} (-K_m^*t)^{(m-n-1)} \quad \text{(Eq. 33)}$$

which can be written more simply as:

$$Q = -\frac{dW}{dt} = mK_m^*W_0(1 - K_m^*t)^{(m-1)} \quad \text{(Eq. 34)}$$

which, after integration, can be written:

$$\left(\frac{W}{W_0}\right)^{1/m} = 1 - K_m^*t \quad \text{(Eq. 35)}$$

As expected, since there is no size distribution effect (2), this equation predicts that the powder will dissolve strictly according to the cube root or square root law.

When the powder is monodisperse, $\mu = \ln a_0$ and Eq. 12 becomes:

$$K_m^* = e^{-(3/m)\ln a_0}K_m = a_0^{-3/m}K_m \quad \text{(Eq. 36)}$$

Equations 11 and 36 then give, for spherical particles[3]:

$$K_m^* = a_0^{-3/m}(6/\rho\pi)^{1/m}k_m = w_0^{-1/m}k_m \quad \text{(Eq. 37)}$$

When $k_m = w_0^{1/m} K_m^*$ (from Eq. 37) is inserted in Eq. 1:

$$\left(\frac{w}{w_0}\right)^{1/m} = 1 - K_m^*t \quad \text{(Eq. 38)}$$

A comparison of Eqs. 38 and 35 shows that, for a monodisperse powder, the specific dissolution rate parameter, K_m^*, is common to both multiparticulate (Eq. 35) and single-particle dissolutions (Eq. 38). It has the dimension of time^{-1} for both single-particle models ($m = 2$ and 3).

Equation 34 can be written:

$$Q^{1/(m-1)} = (mW_0K_m^*)^{1/(m-1)} - (mW_0)^{1/(m-1)}(K_m^*)^{m/(m-1)}t \quad \text{(Eq. 39)}$$

This equation can be used to obtain an initial estimate of K_m^* from the linear regression of $Q^{1/(m-1)}$ on t. In this way, the intercept value, $(mW_0K_m^*)^{1/(m-1)}$ ($t = 0$), divided by $(mW_0)^{1/(m-1)}$ gives $K_m^{*\,1/(m-1)}$ (Fig. 2).

EXPERIMENTAL

The high precision, flow-through, continuously recording dissolution apparatus used for the dissolution tests was described previously (5). Various amounts of micronized glyburide[4] were exposed in the dissolution cell to pH 7.25 phosphate buffer ($I = 0.05$) at a flow rate of 0.568 ml/sec (~ 0.149-cm/sec linear flow rate) and at a temperature of $37.5 \pm 0.2°$. Values of absorbance were read from the chart recording at 2.5-min intervals. The dissolution rate, Q, was then given as (volumetric flow rate) $\times$ (absorbance)/(absorption coefficient).

The accuracy of the rate data was checked by integration. The amount released, calculated in this way, agreed to within $\pm5\%$ with the amount remaining in the dissolution cell at the end of the experiment (which was about 10% of the initial amount). The lower and upper limits for the nonlinear regression parameters used in the curve fitting were chosen as: $\sigma = 0$–1, $K_m^* = 0$–0.1, $i = 0$–10, and $j = 0$–10. The initial estimate for the rate parameter, K_m^*, was obtained graphically (Eq. 41 and Fig. 2).

RESULTS AND DISCUSSION

For a monodisperse powder, Eq. 39 predicts a linear relationship between $\sqrt{Q}$ and t when the single particles dissolve according to the cube root model ($m = 3$) and a linear relationship between Q and t when they dissolve according to the square root model ($m = 2$).

Significant deviations from linearity were observed when dissolution rate data for micronized glyburide were plotted in either of these ways (Figs. 2–6). Such deviations arise if the powder is not monodisperse or if the single particles do not dissolve according to the single-particle model (Eq. 1).

Under an electron microscope, the micronized glyburide used appeared to be considerably polydisperse. Therefore, the observed deviation from

---

[3] The derivation is also valid for nonspherical particles if the concept of spherical approximations (8) applies.
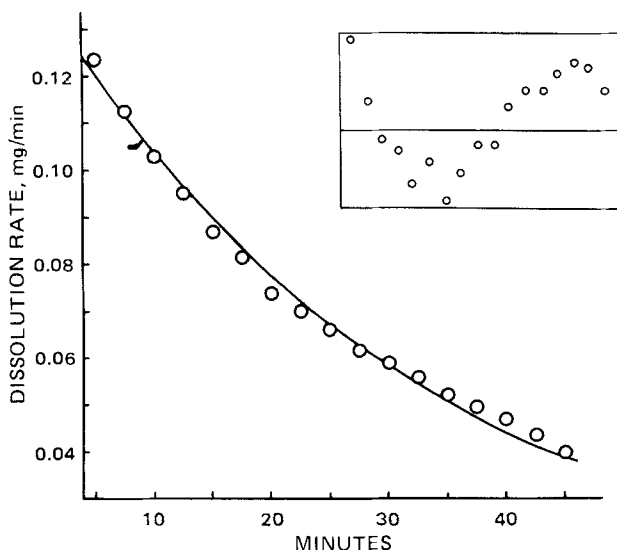[4] Provided by Australian Hoechst Ltd., Sydney, Australia.

Figure 3—*Least-squares fit of the multiparticulate dissolution model (Eq. 30, m = 3) to rate data from the dissolution of 5 mg of micronized glyburide. The model assumes that the effective initial particle-size distribution can be approximated by an ideal log-normal distribution (i = j = ∞, Fig. 1) and that the single particles dissolve according to the cube root model (Eq. 1, m = 3). The inset graph shows a plot of the residuals versus time in arbitrary units.*

Figure 5—*Least-squares fit of the multiparticulate dissolution model (Eq. 30, m = 3) to rate data from the dissolution of 10 mg of micronized glyburide. The model assumes that the effective initial particle-size distribution can be approximated by an ideal log-normal distribution (i = j = ∞, Fig. 1) and that the single particles dissolve according to the cube root model (Eq. 1, m = 3). The inset graph shows a plot of the residuals versus time in arbitrary units.*

linearity in the rate plots can be explained as a particle-size distribution effect if Eq. 1 is assumed to be valid. However, the rate data can also be explained by other single-particle dissolution models in combination with a size distribution effect. Conclusions about the validity of a single-particle model can only be made when the size distribution effect is taken into account.

In a previous study (5) dealing with the dissolution of 60–85-mesh fraction tolbutamide in relation to its particle-size distribution, the dissolution of the single particles accorded well with the cube root model and nearly as well with the square root model. The distribution effect could be evaluated for tolbutamide because of the regular form of its particles. This was not possible for the much smaller micronized glyburide particles, which had very irregular shapes.

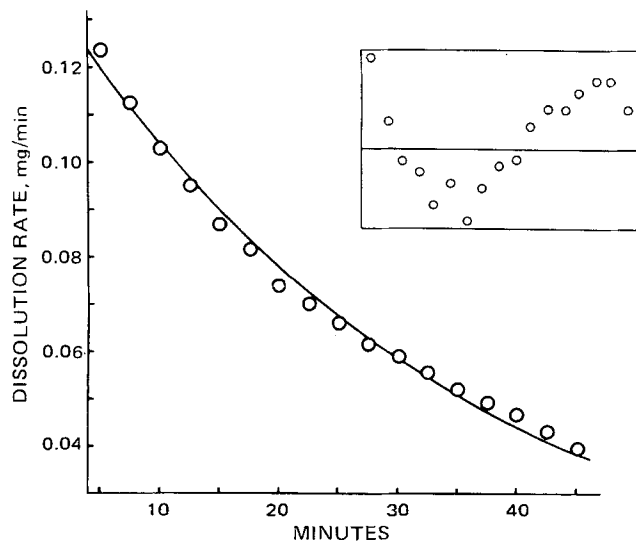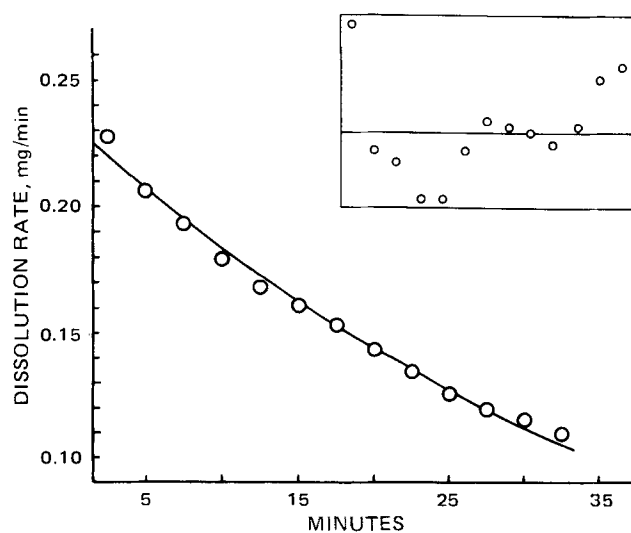**Effective Particle-Size Distribution**—Spherical particles are as-

sumed for the multiparticulate dissolution equations presented. Such particles are usually not encountered in pharmaceutical systems. However, the dissolution of a nonspherical particle can, in most cases, be well approximated by the dissolution of a hypothetical spherical particle (8), particularly under conditions of isotropic dissolution.

A previous paper showed how an equivalent spherical diameter can be calculated from the geometry of simple crystal forms (8). In this way, it is possible to obtain an effective particle-size distribution, i.e., the shape of the distribution of hypothetical spherical particles that approximates the dissolution behavior of the real particles. For tolbutamide, the effective distribution was approximately log-normal (5). Because of the irregular particle shapes, it was not possible to make a priori conclusions about the effective particle-size distribution for glyburide. In these investigations, the distribution was assumed to be log-normal, consistent with previous results (5) and the fact that powders often have log-normal particle-size distribution (9, 10). Therefore, the distribution in Fig. 1 il-
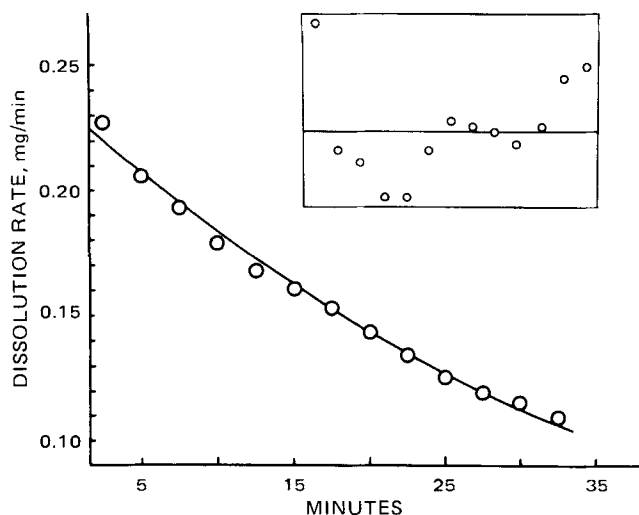

Figure 4—*Least-squares fit of the multiparticulate dissolution model (Eq. 29, m = 3) to rate data from the dissolution of 5 mg of micronized glyburide. The model assumes that the effective initial particle-size distribution can be approximated by a log-normal distribution truncated at both ends (Fig. 1) and that the single particles dissolve according to the cube root model (Eq. 1, m = 3). The inset graph shows a plot of the residuals versus time in arbitrary units.*

Figure 6—*Least-squares fit of the multiparticulate dissolution kinetic model (Eq. 29, m = 3) to rate data from the dissolution of 10 mg of micronized glyburide. The model assumes that the effective initial particle-size distribution can be approximated by a log-normal distribution truncated at both ends (Fig. 1) and that the single particles dissolve according to the cube root model (Eq. 1, m = 3). The inset graph shows a plot of the residuals versus time in arbitrary units.*

Table I—Least-Squares Estimates of Rate and Distribution Parameters Obtained from Nonlinear Regression Analysis of Data from the Dissolution of Micronized Glyburide, Using Various Models for Multiparticulate Dissolution Kinetics[a]

W_0, mg	Parameter	Square Root Model ($m = 2$)			Cube Root Model ($m = 3$)		
		Eq. 30[b]	Eq. 31[c]	Eq. 29[d]	Eq. 30[b]	Eq. 31[c]	Eq. 29[d]
5	K_m^*, min^{-1}	0.02858 (6.39)	0.02858 (5.12)	0.02859 (6.51)	0.02367 (4.55)	0.02367 (4.44)	0.02449 (3.96)
	σ	0.4759 (2.93)	0.4760 (2.70)	0.4760 (3.28)	0.6184 (2.47)	0.6184 (2.11)	0.6315 (1.71)
	i	∞	∞	5.136	∞	∞	2.364
	j	∞	5.299	5.655	∞	9.807	4.172
	r^e	0.9935	0.9935	0.9935	0.9952	0.9952	0.9954
10	K_m^*, min^{-1}	0.02633 (7.18)	0.02633 (10.6)	0.02633 (9.35)	0.02147 (9.45)	0.02147 (4.74)	0.02176 (4.03)
	σ	0.4955 (3.20)	0.4956 (7.24)	0.4955 (5.14)	0.6374 (3.29)	0.6374 (2.03)	0.6446 (1.89)
	i	∞	∞	8.912	∞	∞	4.577
	j	∞	5.299	6.732	∞	7.060	4.200
	r^e	0.9938	0.9938	0.9938	0.9957	0.9957	0.9958

[a] Values in parentheses are relative standard deviations (percent). [b] Initial size distribution is considered ideal ($i = j = \infty$, Fig. 1). [c] Initial size distribution is truncated at the upper end ($i = \infty$, $j < \infty$, Fig. 1). [d] Initial size distribution is truncated at both ends (Fig. 1). [e] Correlation coefficient.

lustrates a log-normal approximation to the effective particle-size distribution. The initial particle diameters, a_0 (Eq. 2), are the diameters of the hypothetical spherical particles that approximate the dissolution of the real nonspherical particles.

If the lower and upper truncation parameters, i or j, are finite, the log-distribution is said to be truncated; otherwise, it is ideal.

Regression Parameters—In a discussion of size distribution effects in multiparticulate dissolution, it was pointed out that the intrinsic dissolution profile does not depend on the actual size of the particles (a_0) but on the shape of their distribution (2). For the same reason, it is not possible to determine by regression analysis the scale parameter, μ, as might be erroneously expected from the appearance of Eq. 28. If, in fact, this equation is used to obtain least-squares estimates of μ and K_m, these values would not be unique. Any other of the infinite combinations of the two parameters that give the same value of K_m^* (Eq. 12) will, according to Eq. 13, result in the same fit (for the same values of σ, i, and j). Therefore, the regression analysis can only provide estimates of the dimensionless distribution parameters σ, i, and j, which define the shape of the initial distribution, and K_m^*. The scale or position of the distribution, given by μ, is hidden in the specific dissolution rate parameter, K_m^* (Eq. 12).

Curve Fitting—Equation 29 was fitted by least squares to dissolution rate data from dissolution of 5 and 10 mg of micronized glyburide[5]. The fitting was done using FUNFIT, an interactive time-sharing program for general nonlinear regression, written by the author[6].

The estimates obtained for the truncation parameters, i and j (Table I, Eq. 29), were all larger than 2 and usually exceeded 4, indicating that the effective initial particle-size distribution (Fig. 1) was close to ideal. It was shown earlier that the effect on the dissolution profile of the lower truncation parameter, i, is negligible (1). Simulation studies also show that the influence of an increase in the upper truncation parameter, j, becomes insignificant when j is larger than 2. Therefore, it is expected from the values of i and j obtained using Eq. 29 that the simpler model, Eq. 30, which assumes an ideal distribution ($i = j = \infty$), should fit the same data nearly as well.

The values in Table I and the curves fitted in Figs. 3–6 confirm this expectation. There does not seem to be any significant difference in the K_m^*, σ, or r values for the two models. The residual plots in Figs. 3–6 also seem to be very similar. Equation 31 (upper truncation) and Eq. 32 (lower truncation) also gave similar results (and, therefore, they have not been included).

Choice of Mathematical Model—In agreement with the general principles of mathematical modeling, Eq. 30 should be considered as the model that best describes the dissolution of the micronized glyburide. It is the simplest of the models, containing only the two parameters K_m^* and σ, and fits the dissolution data just as well as the other models that contain more parameters (i and j).

It also is clear (Table I) that the multiparticulate dissolution model based on the cube root model (Eq. 1, $m = 3$) agrees best with the dissolution data for either a truncated or ideal distribution using either 5 or 10 mg of powder (Table I). Of the eight multiparticulate models investigated, it can be concluded that the following equation:

$$\frac{dW}{dt} = -3K_3^* W_0 \sum_{n=0}^{2} \binom{2}{n} (-K_3^* t)^{(2-n)} \times \left\{ 1 - F\left[\frac{1}{\sigma} \ln(K_3^* t) - n\sigma \right] \right\} e^{(n^2-9)\sigma^2/2} \quad \text{(Eq. 40)}$$

which can be written in integrated form as:

$$\frac{W}{W_0} = \sum_{n=0}^{3} \binom{3}{n} (-K_3^* t)^{(3-n)} \times \left\{ 1 - F\left[\frac{1}{\sigma} \ln(K_3^* t) - n\sigma \right] \right\} e^{(n^2-9)\sigma^2/2} \quad \text{(Eq. 41)}$$

best describes the dissolution kinetics of the micronized glyburide. Either of these two equations uniquely characterizes the dissolution behavior in terms of the rate parameter, K_3^*, and the distribution parameter, σ.

It appears from the residual plots in Figs. 3–6 that there is a serial correlation between the residuals. The Durbin–Watson statistic indicates ($\alpha < 0.05$) that this correlation is significant (11). Systematic deviation can be caused by nonrandom experimental errors. It can also be caused by a significant departure from the assumed single-particle dissolution model (Eq. 1) or by a deviation from log-normality. The residual values are, however, so small in relation to the accuracy of the experimental technique that the correlation seems of little importance.

The specific dissolution rate parameter, K_3^*, theoretically should be independent of the initial amount used, W_0, but this condition was only approximately true. Values of the rate parameter, K_m^*, obtained for $W_0 = 10$ mg were consistently lower than for $W_0 = 5$ mg (Table I). The dissolution models consider dissolution under complete sink conditions, i.e., conditions where there is no interaction between the dissolving particles. When using 10 mg of the very fine powder, it was not possible to load the dissolution cell with a single "layer" of particles in such a way that dissolved drug from any particle did not pass over other particles. The slightly larger K_m^* values observed when less powder was used in the cell agree with an expected smaller particle interaction.

Characterization and Quality Control of Drug Powders—Previous approaches to characterizing the dissolution properties of drug powders have been based on equations describing monodisperse systems. The so-called "dissolution rate constant" sometimes evaluated using such equations will often not characterize the dissolution behavior because the size distribution effect is not taken into account. This is particularly true for pharmaceutical systems, since these systems frequently involve fine, highly polydisperse powders.

The use of nonlinear regression analysis to evaluate the specific dissolution rate parameter, K_m^*, and the distribution parameter, σ, represents a more exact and meaningful approach.

The properties of K_m^* make its interpretation particularly useful. These properties are best understood in relation to the concepts of time scaling and the intrinsic dissolution profile (2) from which the following conclusion can be made:

If K_m^* is changed by a factor α, then the time for complete dissolution, or the time for any particular fraction to dissolve, is changed by a factor of $1/\alpha^7$.

The distribution parameter, σ, is a single measure of how polydisperse

---

[5] The initial data point(s) ($t = 0$ and 2.5 min) was not considered in the curve fitting because of irregularities due to initial adjustments of the solvent flow rate.

[6] The program is available on tape from the author together with a listing of the subroutines specifying the multiparticulate models (Eqs. 29–31).

[7] For example, if it takes x min for a powder to dissolve, e.g., 30% for a given K_m^* value, then it will take the powder $x/2$ min to dissolve to the same extent if the value of K_m^* is doubled (see Fig. 1 in Ref. 2).

a powder is, or more exactly, how much the dissolution behavior deviates from what would be expected if the powder were completely monodisperse. A value close to zero characterizes a nearly monodisperse powder, while higher values indicate increasing "degrees of dispersion." Probably, the most important property of σ is that it is a measure of how long it takes the last fraction of a polydisperse powder to dissolve. For example, it is seen from Eq. 16 that the time for complete dissolution increases exponentially with σ. For this reason, a significant correlation probably exists between σ and systemic availability for very slightly soluble drugs that exhibit low systemic availability due to dissolution rate-limited absorption. Research in this area should be of considerable pharmaceutical interest.

Although the multiparticulate dissolution model (Eqs. 40 and 41) defining K_m^* and σ may seem complex, the interpretation of these parameters is simple and they can be readily obtained. The experimental technique used requires a high precision, flow-through dissolution apparatus that is easy to standardize [e.g., the apparatus described in Ref. 5 or other suitable flow-through system (12)] in combination with a nonlinear regression program.

The method could well become established as a routine procedure in quality control, and further investigation could result in improved standards for drug dissolution.

REFERENCES

(1) P. Veng Pedersen and K. F. Brown, J. Pharm. Sci., 64, 1192 (1975).

(2) Ibid., 64, 1981 (1975).

(3) W. I. Higuchi, E. I. Rowe, and E. N. Hiestand, J. Pharm. Sci., 52, 162 (1963).

(4) J. T. Carstensen and M. Patel, ibid., 64, 1770 (1975).

(5) P. Veng Pedersen and K. F. Brown, ibid., 65, 1442 (1976).

(6) A. Hixson and J. Crowell, Ind. Eng. Chem., 23, 923 (1931).

(7) P. J. Niebergall, G. Milosovich, and J. E. Goyan, J. Pharm. Sci., 52, 236 (1963).

(8) P. Veng Pedersen and K. F. Brown, ibid., 65, 1437 (1976).

(9) G. Herdan and M. L. Smith, "Small Particle Statistics," Elsevier, New York, N.Y., 1953.

(10) T. Hatch and S. P. Choate, J. Franklin Inst., 207, 369 (1929).

(11) J. Durbin and G. S. Watson, Biometrica, 37, 409 (1950).

(12) "Dissolution Technology," L. J. Leeson and J. T. Carstensen, Eds., Industrial Pharmaceutical Technology, APhA Academy of Pharmaceutical Sciences, Washington, D.C., 1974.

Sensitive Assay Procedure for Ethambutol Hydrochloride via Charge Transfer Complex Formation

HENRY S. I. TAN x, ERIC D. GERLACH, and ANTHONY S. DIMATTIO

Abstract □ The charge transfer complex formation between ethambutol and iodine was investigated and utilized as the basis for a sensitive spectrophotometric procedure for ethambutol and its dosage forms. The solutions exhibited blue-shifted iodine bands at 293 and 360 nm. A Job's plot of corrected absorbance against the mole ratio of ethambutol to iodine indicated a 1:2 drug–iodine ratio. At 293 nm, the absorbance was linear ($r = 0.9998$) over the 0.25–15-μg/ml concentration range, but the concentration range for best accuracy is 1.6–5.8 μg/ml. The method can be applied successfully to the analysis of commercially available ethambutol tablets.

Keyphrases □ Ethambutol—spectrophotometric analysis using charge transfer complex formation, prepared samples and commercial tablets □ Spectrophotometry—analysis using charge transfer complex formation, ethambutol in prepared samples and commercial tablets □ Charge transfer complex formation—spectrophotometric analysis of ethambutol in prepared samples and commercial tablets □ Antibacterials—ethambutol, spectrophotometric analysis using charge transfer complex formation, prepared samples and commercial tablets

Ethambutol is a new antitubercular drug included in USP XIX (1). Being a relatively new drug, few procedures have been reported for its determination as a drug substance or in commercial dosage forms. The official assay procedure involves a nonaqueous titration with perchloric acid titrant (1).

Quantitative analyses of small quantities of ethambutol have been based on the chelation properties of the drug with copper in aqueous or nonaqueous media (2, 3). A reineckate method and an acid–dye technique using bromthymol blue were also reported (4, 5). However, these procedures are not feasible for the analysis of microquantities of the drug in biological fluids.

Amines and alcohols are lone-pair (n) electron donors and can interact strongly with sacrificial electron acceptors such as iodine to form charge transfer complexes (6). Recently, a study on charge transfer complexes of iodine with alkaloids was reported (7). This paper reports the charge transfer complex formation of ethambutol with iodine and its application to drug assay.

EXPERIMENTAL

Apparatus—A UV–visible double-beam spectrophotometer[1] with 1-cm cells and dynode voltage of 500 v (slit width 0.80–0.85 mm) and an analytical balance[2] were used.

Materials and Reagents—Ethambutol hydrochloride[3] and 8×10^{-4} M iodine[4] (resublimed) in anhydrous chloroform[4] were used. Other reagents were analytical grade.

Ethambutol Base—Ethambutol hydrochloride (1 g) was dissolved

---

[1] Beckman Acta V, Beckman Instruments Inc., Fullerton, Calif.
[2] Mettler model H-18, Mettler Instruments Co., Princeton, N.J.
[3] Lederle Laboratories, Pearl River, N.Y.
[4] Fisher Scientific Co., Pittsburgh, Pa.